Fatigue Prediction for Composite Materials and Structures

Omar SALOMON*, Fernando RASTELLINI, Sergio OLLER and Eugenio OÑATE
CIMNE (International Center for Numerical Methods in Engineering)
Building C-1, Campus Nord UPC -C/ Gran Capitán s/n
08034 Barcelona
SPAIN

* salomon@cimne.upc.edu

ABSTRACT

The objective of this paper is to present a new computational methodology for predicting the durability of structures made of composite materials based on epoxy matrix with long carbon fibres.

To analyse the behaviour of composite materials an Enhanced Serial-Parallel constitutive model (ESP model) is developed assuming components behave as parallel materials in the fibres alignment direction and as serial materials in orthogonal directions. It allows equal component strains in the fibre direction and equal stresses in the transverse directions. The ESP model brings answers on the non-linear behaviour of composites, where Classical Micro-mechanics Formulas are restricted to their linear elastic part. Constitutive tensors of the composite materials are obtained from mechanical properties and internal variables of their components within a continuum framework. Anisotropy and different constitutive models (plasticity, damage and fatigue) for each phase are considered.

The fatigue prediction model is based in a continuum mechanic stress life approach for each of the component materials. S-N curves are proposed for each phase. A cumulative fatigue damage index is used to update the mechanical properties of the components and with these properties update layers properties and compute residual stiffness of the laminate.

Constitutive models for the composite materials have been implemented into a general purpose finite element code (COMET) and a user friendly interface for composite material data input in a pre-post processing module (GiD) has been developed. The methodology is validated using experimental data from tests on CFRR composite material samples.

1.0 INTRODUCTION

Fatigue is defined as "the process of permanent, progressive and localized structural change which occurs to a material point subjected to strains and stresses of variable amplitudes which produces cracks leading to total failure after a certain number of cycles" and it is the main cause of failure of machine parts in service, in mechanisms and structural elements in aeronautics, naval and automotive industries. Fatigue failure can occurs under load conditions well below the strength limit of the material. Typically, a progressive loss of strength occurs depending on the number of stress/strain cycles, reversion index, load amplitude, etc. This loss of strength induce the material to inelastic behaviour, which may be interpreted as micro-cracking followed by crack coalescence leading to the final collapse of structural parts.

Salomon, O.; Rastellini, F.; Oller, S.; Oñate, E. (2005) Fatigue Prediction for Composite Materials and Structures. In *Evaluation, Control and Prevention of High Cycle Fatigue in Gas Turbine Engines for Land, Sea and Air Vehicles* (pp. 31-1 – 31-22). Meeting Proceedings RTO-MP-AVT-121, Paper 31. Neuilly-sur-Seine, France: RTO. Available from: http://www.rto.nato.int/abstracts.asp.

Report Documentation Page

Form Approved
OMB No. 0704-0188

1. REPORT DATE	2. REPORT TYPE	3. DATES COVERED
01 OCT 2005	**N/A**	**-**

4. TITLE AND SUBTITLE	5a. CONTRACT NUMBER
Fatigue Prediction for Composite Materials and Structures	5b. GRANT NUMBER
	5c. PROGRAM ELEMENT NUMBER
6. AUTHOR(S)	5d. PROJECT NUMBER
	5e. TASK NUMBER
	5f. WORK UNIT NUMBER
7. PERFORMING ORGANIZATION NAME(S) AND ADDRESS(ES) **CIMNE (International Center for Numerical Methods in Engineering) Building C-1, Campus Nord UPC -C/ Gran Capitán s/n 08034 Barcelona SPAIN**	8. PERFORMING ORGANIZATION REPORT NUMBER
9. SPONSORING/MONITORING AGENCY NAME(S) AND ADDRESS(ES)	10. SPONSOR/MONITOR'S ACRONYM(S)
	11. SPONSOR/MONITOR'S REPORT NUMBER(S)

12. DISTRIBUTION/AVAILABILITY STATEMENT
Approved for public release, distribution unlimited

13. SUPPLEMENTARY NOTES
See also ADM202115, RTO-MP-AVT-121. Evaluation, Control and Prevention of High Cycle Fatigue in Gas Turbine Engines for Land, Sea and Air Vehicles., The original document contains color images.

14. ABSTRACT

15. SUBJECT TERMS

16. SECURITY CLASSIFICATION OF:			17. LIMITATION OF ABSTRACT	18. NUMBER OF PAGES	19a. NAME OF RESPONSIBLE PERSON
a. REPORT	b. ABSTRACT	c. THIS PAGE			
unclassified	**unclassified**	**unclassified**	**UU**	**22**	

This study is based on the hypothesis that fatigue damage is essentially of the same nature as mechanical damage and can be described via an internal variable allowing the adequate treatment of the accumulation and localization of dislocations, therefore the theoretical structure of continuum mechanics (such as plasticity and damage) is suitable for the study of non linear fatigue problems. The inelastic theories of plasticity and/or damage solve the problem of material behaviour beyond the elastic range and both theories allow the study of the change in strength that a material point suffers by inelastic effects, however they are not sensitive to cyclic load effects. In this work the standard inelastic theories are modified to account for fatigue effect coupled with non-fatigue behaviour [1].

Concerning composite materials, in this work, a numerical model to assess the constitutive non-linear behaviour of a unidirectional lamina is conceived [2]. It is based on the appropriate management of the constitutive models of component phases within a continuum framework. With such aim, a strategy is developed to decouple phases that may also consider possible inelastic strains and/or elastic degradation of the stiffness based on previous development of the authors [3], [4]. Input data are the mechanical properties of each component (i.e.: fibres and matrix in case of fibre-reinforced laminates) and its distribution inside the composite. This methodology of mixing components with the strategy for phases decoupling allow each component to retain, unchanged, its original constitutive law (isotropic or anisotropic, linear or non-linear) while conditioning the composite global response. Different constitutive models (plasticity, damage, fatigue, creep, etc.) for each phase may be taken into account.

The composite model (for a single lamina) is combined with classical lamination theory to describe laminates consisting of unidirectional continuously reinforced layers. Its relative simplicity and the resulting numerical efficiency make this approach well suited for implementation as a material model in Finite Element programs for studying the elastoplastic response of structures or components made of continuously reinforced or laminated composites. The previous mentioned fatigue model is applied to each component in order to obtain the durability of the whole composite laminate.

2.0 CONTINUUM MECHANICAL MODEL FOR FATIGUE ANALYSIS

It is assumed that each point of the solid follows a damage-elasto-plastic constitutive law with the stress (S) evolution depending on the free elastic strain variable (E^e) and a set of internal plastic and damage variables $\boldsymbol{q}=\{\boldsymbol{\alpha}^p,d\}=\{\boldsymbol{E}^p,\ \kappa^p,d=\kappa^d\ \}$, were $\boldsymbol{E}^p$ and $\kappa^{ini}\leq(\kappa=\kappa^p+\kappa^d)\leq 1$ represent the plastic part of the strain and a unit normalized dissipation composed by the plastic plus damage parts, respectively.

The free energy for isothermal, isentropic and adiabatic processes and for small elastic strains and large plastic strains is written in the reference configuration, accepting the additivity of its elastic Ψ^e and plastic Ψ^p parts, as

$$\Psi=\Psi^e(E^e_{ij},d)+\Psi^p(\alpha^p_i)=(1-d)\frac{1}{2m^o}\left[E^e_{ij}\,\mathrm{C}^o_{ijkl}\,E^e_{kl}\right]+\Psi^p(\alpha^p_i) \tag{1}$$

where E^e is elastic Green strain tensor, m^0 is the material density, $d=\kappa^d$ is the internal mechanical damage variable for the damage processes $d^{ini}\leq\left(d=\kappa^d\right)\leq 1$ with the initial value $d^{ini}\equiv\kappa^{ini}$ provided by the defect level, and C^0_{ijkl} the initial constitutive tensor. The stress tensor in the reference configuration S_{ij} can be expressed as

$$S_{ij} = m^o \frac{\partial \Psi}{\partial E^e_{ij}} = (1-d)\, C^o_{ijkl}\, E^e_{kl} \tag{2}$$

For the plastic behaviour, the general forms of the yield F and potential G plastic functions take into account the influence of the current stress state, the internal plastic variables, and other variables such as the number of cycles N:

$$\begin{aligned} F(S_{ij},\kappa) &= f(S_{ij}) - K(S_{ij},\kappa,N) \\ G(S_{ij}) &= g(S_{ij}) = \text{constant.} \end{aligned} \tag{3}$$

where $f(S_{ij})$ and $g(S_{ij})$ are the uniaxial equivalent stress functions, $K(S_{ij},\kappa,N)$ is the strength threshold (see Figure 1). All the internal variables at current time t are obtained by means of an integration process $\alpha_i^p = \int_0^t \dot{\alpha}_i^p\, dt$, starting from its evolution law $\alpha_i^p = \dot{\lambda}\, H_i^p(S_{kl},\alpha_k^p)$, where λ is the plastic consistent factor.

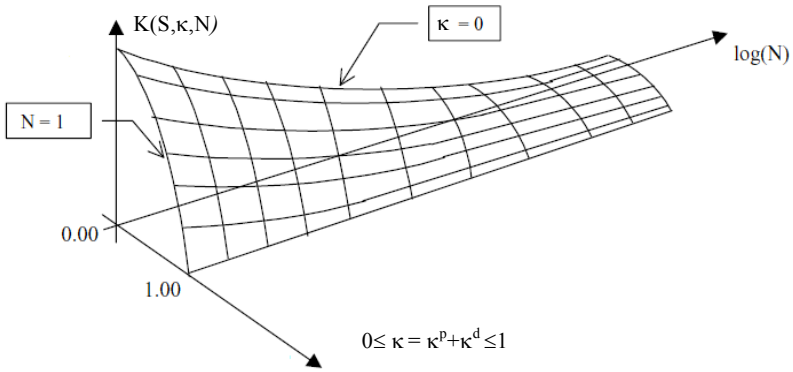

Figure 1: Uniaxial strength threshold for a symbolic material.

The damage function is defined as

$$G^D(S_{ij},\kappa) = \bar{S}(S_{ij}) - K(S_{ij},\kappa,N) \tag{4}$$

where $\bar{S}(S_{ij})$ is the uniaxial equivalent stress function in the undamaged space, $K(S_{ij},\kappa,N)$ is the same strength threshold as in (3) and $\kappa^d = d = \int_0^t \dot{d}\, dt$ the damage internal variable with an evolution defined as $d = \mu\, H^D(S_{kl},d)$, where μ is the consistency damage factor. In both, (3) and (4), the normalized dissipation is defined as $\kappa = \kappa^p + \kappa^d = \left(\Xi^p + \Xi^d\right)/\Xi^{\max}$, where Ξ^p, Ξ^d, $\Xi^{\max}$ are the Clausius-Duhem dissipation for the current plastic, damage process and its maximum capacity of the solid dissipation at each point, respectively.

The effect of the number of cycles on the plastic and/or damage consistency conditions ($\dot{F}=0$, $\dot{G}^D=0$) is introduced as follows,

$$f(S_{ij}) - \underbrace{K(S_{ij},\kappa).f_{red}(N,S_{med},R)}_{K(S_{ij},R,N)} = 0 \tag{5}$$

$$\bar{S}(S_{ij}) - \underbrace{K(S_{ij},\kappa).f_{red}(N,S_{med},R)}_{K(S_{ij},R,N)} = 0 \tag{6}$$

where $0 \le f_{red} \le 1$ represent the unit normalized reduction part of the strength threshold K —plastic and/or damage strength evolution— by load cyclic effect.

S-N Curves

Stress-Nº of cycles (*S-N*) curves are experimentally obtained by subjecting identical smooth specimens to cyclic harmonic stresses and establishing their life span measured in number of cycles. The curves depend on the level of the maximum applied stress and on the ratio between the lowest and the highest stresses ($R = S_{\min} / S_{\max}$). In previous works ([1],[5],[6]) an exponential function to approach steel and aluminium experimental *S-N* curves was proposed. This function depends on and is capable of dealing with any value of the ratio between minimum and maximum stress. However, it is a bit difficult to adjust its parameters to obtain a good approximation to experimental curves, which are usually not defined over the whole life-span of the material. Instead of using such an exponential function, here the experimental data is introduced by points in a table-like mode.

Usually, *S-N* curves are obtained for a fully reversed stress state ($R = S_{\min} / S_{\max} = -1$) by rotating bending fatigue tests. This zero mean stress is however not typical of real industrial components working under cyclic loads. Based on the actual value of the *R* ratio and a basic value of the endurance stress *Se* (for *R = -1*) the model proposed postulates a threshold stress S_{th}. The meaning of S_{th} is that of an endurance stress limit for a given value of $R = S_{\min} / S_{\max}$; if the actual value of *R* is *R*= -1 then, $S_{th} = S_e$.

$$\begin{aligned} S_{th} &= S_e + (S_u - S_e)\cdot(0.5 + 0.5\cdot R)^{STHR1} \longrightarrow abs(R) \le 1 \\ S_{th} &= S_e + (S_u - S_e)\cdot(0.5 + 0.5/R)^{STHR2} \longrightarrow abs(R) \ge 1 \end{aligned} \tag{7}$$

STHR1 and *STHR2* are material parameters that need to be adjusted according to experimental tests.

Cyclic Strength Reduction Function

The *S-N* curves proposed in the previous section are fatigue life estimators for a material point with a fixed maximum stress and a given ratio *R*. If, after a number of cycles lower than the cycles to failure, the constant amplitude cyclic loads giving that maximum stress $S_{\max}$ (and ratio *R*) are removed, some change in S_u is expected due to accumulation of fatigue cycles. In order to describe the variation of S_u the following function is proposed:

$$\begin{aligned} fred(R, Ncycles) &= \exp(-B0\cdot(\log 10(Ncycles))^{BETAF}) \\ B0 &= -\log 10(S_{\max}/S_u)/(\log 10(N_F))^{BETAF} \end{aligned} \tag{8}$$

BETAF is a material parameter and N_F the number of cycles to failure.

Time Advancing Strategy

An advantage of the methodology presented consists in the way the loading is applied. In a mechanical problem each load is applied in two intervals, in the following order (see Figure 2),

-**Tracing load**, (described by "ai" periods on Figure 2). It is used to obtain the stress ratio $R = S_{\min} / S_{\max}$ at each integration point, following the load path during several cycles until the R relationship tends to a constant value. This occurs when the following norm is satisfied,

$$\eta = \sum_{GP} \left\| \frac{R_{GP}^{i+1} - R_{GP}^{i}}{R_{GP}^{i+1}} \right\| \rightarrow 0 \qquad (9)$$

where $R_{GP}^{i} = S_{\min} / S_{\max}\big|_{GP}^{i}$ is computed at each Gauss interpolation point for the load increment "i".

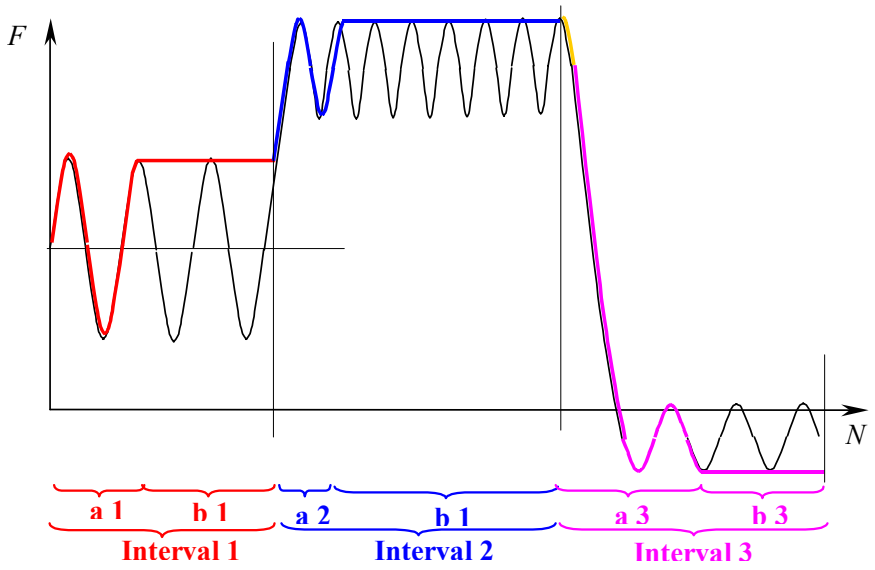

Figure 2: Schematic time advancing loads representation. ai describes the tracking load domain on the i interval. bi describes the enveloping load domain on the same i interval.

-**Enveloping load**, (described by "bi" periods on Figure 2). After the first tracing load interval (ai), the number of cycles N is increased while keeping constant the maximum applied load (thick line in Figure 2) and the stress ratio R. In this new load interval, the variable is not the load level (kept constant) but the number of cycles.

This two-stages strategy allows a very fast advance in the time loading. A new interval with the two stages explained should be added for each change in the loading level.

3.0 CONSTITUTIVE MODEL FOR FIBRE REINFORCED LAMINA

In composite materials each component makes the composite behaviour dependent on its own constitutive law according to its volumetric participation. In addition, the components morphological distribution inside the composite becomes essential, giving better properties to the composite material than its component parts. Classical Mixing Theory (CMT), also known as Rule of Mixtures (ROM), takes into account the volumetric contribution of components but not its morphological distribution. Therefore, CMT can be only useful to obtain basic properties of composite materials assuming parallel behaviour (components with same strains in all directions). This hypothesis is a strong limitation for the use of CMT to predict the behaviour of most composites and consequently modifications to this theory are always required.

In the late 1970s, a simple micromechanically-based constitutive relation for composite materials has been developed [8]. This model consists of aligned continuous fibres embedded in an elastoplastic matrix. Approximate stress and strain fields are prescribed for matrix and fibres, strain coupling in the axial direction and stress coupling for all other stress and strain components [9]. The model account for load sharing (fibres-matrix) in the axial direction, but fibres do not interact with the deformation of the matrix in any other direction, leading to a response that underestimate the transverse and shear stiffness.

To overcome these limitations, a general numerical procedure for non-linear constitutive behavior simulation of the unidirectional laminas is developed. This model is able to capture the simultaneous serial and parallel behaviours, which takes place inside the composite, independently of loading directions. It is based on the appropriate management of the constitutive models of component phases within a continuum framework. With such an aim, a strategy is developed to decouple phases that may also contribute possible inelastic strains and/or elastic degradation of the stiffness. Input data are the mechanical properties of each component (i.e.: fibres and matrix in case of fibre-reinforced laminates) and its distribution inside the composite. This methodology of mixing components with the strategy for phase decoupling allows each component to retain, unchanged, its original constitutive law (isotropic or anisotropic, linear or non-linear) while conditioning the composite global response. Different constitutive models (plasticity, damage, fatigue, creep, etc.) for each phase may be taken into account.

3.1 Definition of Serial and Parallel Parts of Strain/Stress Tensors

The SP model considers that in a certain direction (or directions) the compounding materials behave “in parallel”, while their behaviour is “serial” in the remaining directions. For this reason, it is necessary to define and split the serial and parallel parts of strain and stress tensors.

Different types of serial-parallel mixtures may be considered: from the pure parallel (same strain field for all phases) or the pure serial (same stress field for all phases), up to the cases of parallel behaviour in one direction (fibre reinforced matrices) or in a plane (biphasic laminates). This work is focus on the unidirectional fibres case.

Unidirectional Fibres Case

Being e_1, the director versor that determines the parallel behaviour (fibre direction), and being e_2 and e_3 the director tensors, orthogonal to e_1, that determines the directions where serial behaviour takes place, the parallel projector tensor $\mathbf{N}_P$ may be defined as follows:

$$\mathbf{N}_P = e_1 \otimes e_1 \tag{10}$$

It is a second order tensor that gives the parallel (to fibres) projection of a generic vector v:

$$v_P = \mathbf{N}_P \cdot v \tag{11}$$

It is now defined the 4th-ordered parallel projector tensor $\mathbf{P}_P$:

$$\mathbf{P}_P = \mathbf{N}_P \otimes \mathbf{N}_P \tag{12}$$

The serial projector tensor $\mathbf{P}_S$ is evaluated as its complement:

$$\mathbf{P}_S = \mathbf{I} - \mathbf{P}_P \tag{13}$$

Both tensors allow finding the parallel part of the strain tensor, $\boldsymbol{\varepsilon}_P$:

$$\boldsymbol{\varepsilon}_P = \mathbf{P}_P : \boldsymbol{\varepsilon} \tag{14}$$

and its serial part, $\boldsymbol{\varepsilon}_S$:

$$\boldsymbol{\varepsilon}_S = \mathbf{P}_S : \boldsymbol{\varepsilon} \tag{15}$$

By this mean, the strain state is split into its parallel and serial parts:

$$\boldsymbol{\varepsilon} = \boldsymbol{\varepsilon}_P + \boldsymbol{\varepsilon}_S \tag{16}$$

The stress state may be split analogously:

$$\boldsymbol{\sigma} = \boldsymbol{\sigma}_P + \boldsymbol{\sigma}_S \tag{17}$$

where:

$$\boldsymbol{\sigma}_P = \mathbf{P}_P : \boldsymbol{\sigma} \tag{18}$$

$$\boldsymbol{\sigma}_S = \mathbf{P}_S : \boldsymbol{\sigma} \tag{19}$$

3.2 Hypothesis for the Numerical Modelling

The present numerical model formulation is based on the following hypothesis:

1) Component materials have the same strain in parallel (fibre) direction,
2) and the same stress in serial directions.
3) Composite material response is in direct relation with the volume fractions of compounding materials.

4) Homogeneous distribution of phases is considered.

5) Perfect bonding between components is also considered.

3.3 Equations that Govern the Serial-Parallel Behaviour

Constitutive Equations of Compounding Materials

A general case is considered, with materials that may undergo degradation not only because of plastic strains growth but also because of deterioration or elastic damage in their stiffness:

$$ {}^{m}\boldsymbol{\sigma} = {}^{m}f\left({}^{m}\boldsymbol{\varepsilon}, {}^{m}\boldsymbol{\varepsilon}^{p}, {}^{m}\mathbf{C}^{d}\right) \tag{20} $$

$$ {}^{f}\boldsymbol{\sigma} = {}^{f}f\left({}^{f}\boldsymbol{\varepsilon}, {}^{f}\boldsymbol{\varepsilon}^{p}, {}^{f}\mathbf{C}^{d}\right) \tag{21} $$

As an example, the particular case of additive plasticity is shown:

$$ {}^{m}\boldsymbol{\sigma} = {}^{m}\mathbf{C}^{d} : \left({}^{m}\boldsymbol{\varepsilon} - {}^{m}\boldsymbol{\varepsilon}^{p}\right) $$

$$ {}^{f}\boldsymbol{\sigma} = {}^{f}\mathbf{C}^{d} : \left({}^{f}\boldsymbol{\varepsilon} - {}^{f}\boldsymbol{\varepsilon}^{p}\right) $$

Constitutive equations of compounding materials may be rewritten taking into account the serial and parallel split of strain and stress tensors –eqs. (16) and (17)–:

$$ \begin{bmatrix} {}^{c}\boldsymbol{\sigma}_{P} \\ {}^{c}\boldsymbol{\sigma}_{S} \end{bmatrix} = \begin{bmatrix} {}^{c}\mathbf{C}^{d}_{PP} & {}^{c}\mathbf{C}^{d}_{PS} \\ {}^{c}\mathbf{C}^{d}_{SP} & {}^{c}\mathbf{C}^{d}_{SS} \end{bmatrix} : \begin{bmatrix} {}^{c}\boldsymbol{\varepsilon}_{P} - {}^{c}\boldsymbol{\varepsilon}^{p}_{P} \\ {}^{c}\boldsymbol{\varepsilon}_{S} - {}^{c}\boldsymbol{\varepsilon}^{p}_{S} \end{bmatrix} $$

$$ \text{where:} \begin{cases} {}^{c}\mathbf{C}^{d}_{PP} = \mathbf{P}_{P} : {}^{c}\mathbf{C}^{d} : \mathbf{P}_{P} \\ {}^{c}\mathbf{C}^{d}_{PS} = \mathbf{P}_{P} : {}^{c}\mathbf{C}^{d} : \mathbf{P}_{S} \\ {}^{c}\mathbf{C}^{d}_{SP} = \mathbf{P}_{S} : {}^{c}\mathbf{C}^{d} : \mathbf{P}_{P} \\ {}^{c}\mathbf{C}^{d}_{SS} = \mathbf{P}_{S} : {}^{c}\mathbf{C}^{d} : \mathbf{P}_{S} \end{cases} \quad \text{with: } c = m, f $$

Equilibrium and Compatibility Equations

The equations that define the stress equilibrium and establish the strain compatibility between components arise from the analysis of the previously formulated hypotheses:

Parallel behaviour:

$$ \boldsymbol{\varepsilon}_{P} = {}^{m}\boldsymbol{\varepsilon}_{P} = {}^{f}\boldsymbol{\varepsilon}_{P} \tag{22} $$

$$ \boldsymbol{\sigma}_{P} = {}^{m}k \; {}^{m}\boldsymbol{\sigma}_{P} + {}^{f}k \; {}^{f}\boldsymbol{\sigma}_{P} \tag{23} $$

Serial behaviour:

$$\boldsymbol{\sigma}_S = {}^m\boldsymbol{\sigma}_S = {}^f\boldsymbol{\sigma}_S \tag{24}$$

$$\boldsymbol{\varepsilon}_S = {}^m k \; {}^m\boldsymbol{\varepsilon}_S + {}^f k \; {}^f\boldsymbol{\varepsilon}_S \tag{25}$$

where ${}^m k$ and ${}^f k$ are volume fraction coefficients, fulfilling: ${}^m k + {}^f k = 1$.

3.4 Exposition of the Problem

Given the composite strain state $\boldsymbol{\varepsilon}$ at the present time $(t + \Delta t)$, and known the components internal variables of the previous step (t), find the strain state of the components and also the corresponding stress states at the present time that fulfil the equilibrium, compatibility and constitutive equations described in the previous section.

The following chart point up the known and unknown variables of the problem:

Known variables:	${}^{t+\Delta t}[\boldsymbol{\varepsilon}]$,	free variable
	${}^t[{}^m\alpha]$, ${}^t[{}^f\alpha]$.	internal variables
Unknown variables:	${}^{t+\Delta t}[{}^m\boldsymbol{\varepsilon}]$, ${}^{t+\Delta t}[{}^f\boldsymbol{\varepsilon}]$,	dependent variables
	${}^{t+\Delta t}[{}^m\boldsymbol{\sigma}]$, ${}^{t+\Delta t}[{}^f\boldsymbol{\sigma}]$, ${}^{t+\Delta t}[\boldsymbol{\sigma}]$,	
	${}^{t+\Delta t}[{}^m\alpha]$, ${}^{t+\Delta t}[{}^f\alpha]$.	updated internal variables

Variables ${}^m\alpha$ and ${}^f\alpha$ group all the set of internal variables corresponding to the components, like for example internal variables of damage and/or plasticity that define the materials state:

$${}^m\alpha := \left\{ {}^m\boldsymbol{\varepsilon}^p, {}^m\mathbf{C}^d \right\}$$

$${}^f\alpha := \left\{ {}^f\boldsymbol{\varepsilon}^p, {}^f\mathbf{C}^d \right\}$$

3.5 Algorithm for Compounding Behaviours

It is now introduced the algorithm for the constitutive model of a composite material made up of behaviours of different materials (e.g.: fibre and matrix). It will be seen that the model that sets out constitutes, in fact, a manager of non-linear constitutive models, which combines the hypotheses enunciated for composites with general material models (simple or complex ones).

Each increase of load may cause evolution of the internal variables of the component materials, producing an stress disequilibrium incompatible with the second hypothesis (see section 3.2). This stress disequilibrium constitutes the residue to minimize:

$$\Delta\boldsymbol{\sigma}_S = {}^m\boldsymbol{\sigma}_S - {}^f\boldsymbol{\sigma}_S \tag{26}$$

It is chosen as unknown the total serial strain of one of the materials –in this case the one from the matrix (${}^m\boldsymbol{\varepsilon}_S$)– since the strain of the other material depends on the first one:

$${}^f\boldsymbol{\varepsilon}_S\left({}^m\boldsymbol{\varepsilon}_S\right) = \tfrac{1}{{}^fk}\,\boldsymbol{\varepsilon}_S - \tfrac{{}^mk}{{}^fk}\,{}^m\boldsymbol{\varepsilon}_S \tag{27}$$

$$\Delta\boldsymbol{\sigma}_S\left({}^m\boldsymbol{\varepsilon}_S\right) = {}^m\boldsymbol{\sigma}_S\left({}^m\boldsymbol{\varepsilon}_S\right) - {}^f\boldsymbol{\sigma}_S\left({}^f\boldsymbol{\varepsilon}_S\left({}^m\boldsymbol{\varepsilon}_S\right)\right) \tag{28}$$

The derivative of the objective function (residue) with respect to the unknown:

$$\frac{\partial\left[\Delta\boldsymbol{\sigma}_S\right]}{\partial\,{}^m\boldsymbol{\varepsilon}_S} = \frac{\partial\left[{}^m\boldsymbol{\sigma}_S - {}^f\boldsymbol{\sigma}_S\right]}{\partial\,{}^m\boldsymbol{\varepsilon}_S} = \frac{\partial\,{}^m\boldsymbol{\sigma}_S}{\partial\,{}^m\boldsymbol{\varepsilon}_S} - \frac{\partial\,{}^f\boldsymbol{\sigma}_S}{\partial\,{}^f\boldsymbol{\varepsilon}_S} : \frac{\partial\,{}^f\boldsymbol{\varepsilon}_S}{\partial\,{}^m\boldsymbol{\varepsilon}_S} \tag{29}$$

gives the expression of the Jacobian:

$$\begin{aligned}\mathbf{J} = \left.\frac{\partial\left[\Delta\boldsymbol{\sigma}_S\right]}{\partial\,{}^m\boldsymbol{\varepsilon}_S}\right|_{{}^m\boldsymbol{\varepsilon}_S=\left[{}^m\boldsymbol{\varepsilon}_S\right]^k} &= \frac{\partial\left[{}^m\boldsymbol{\sigma}_S\right]^k}{\partial\,{}^m\boldsymbol{\varepsilon}_S} - \frac{\partial\left[{}^f\boldsymbol{\sigma}_S\right]^k}{\partial\,{}^f\boldsymbol{\varepsilon}_S} : \frac{\partial\,{}^f\boldsymbol{\varepsilon}_S}{\partial\,{}^m\boldsymbol{\varepsilon}_S} \\ &= \left[{}^m\mathbf{C}^T_{SS}\right]^k - \left[{}^f\mathbf{C}^T_{SS}\right]^k : \left(-\tfrac{{}^mk}{{}^fk}\,\mathbf{I}\right) \\ &= \left[{}^m\mathbf{C}^T_{SS}\right]^k + \tfrac{{}^mk}{{}^fk}\left[{}^f\mathbf{C}^T_{SS}\right]^k\end{aligned} \tag{30}$$

that it is used to update the unknown at each local iterative step of the Newton-Raphson method:

$$\left[{}^m\boldsymbol{\varepsilon}_S\right]^{k+1} = \left[{}^m\boldsymbol{\varepsilon}_S\right]^k - \mathbf{J}^{-1} : \left[\Delta\boldsymbol{\sigma}_S\right]^k \tag{31}$$

Note that, from now on, when $\left[\bullet\right]^k$ is shown, it should be understood ${}^{t+\Delta t}\left[\bullet\right]^k$.

Step 1. Initial Approximation.

The initial approximation of the unknown can be established when considering that the strain increment maintains the tangent evolution of the previous step:

- First, the constitutive models of each material are evaluated to determine their constitutive tangent tensors corresponding to the previous step.

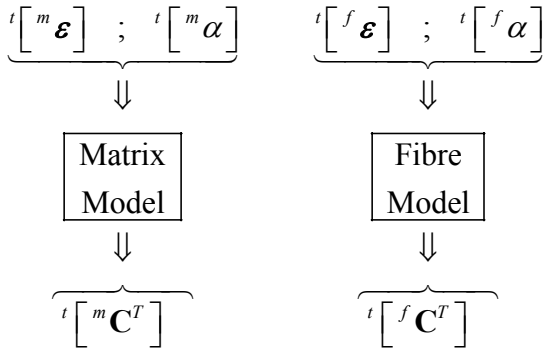

- Then, the increment of the unknown is determined supposing that the total strain increment is distributed among constituent materials according to their previous step tangent stiffness:

$$
\begin{aligned}
{}^{t}\left[\boldsymbol{\varepsilon}_S\right] &= {}^{m}k\ {}^{t}\left[{}^{m}\boldsymbol{\varepsilon}_S\right] + {}^{f}k\ {}^{t}\left[{}^{f}\boldsymbol{\varepsilon}_S\right] \\
\left[\Delta\boldsymbol{\varepsilon}_S\right] &= {}^{t+\Delta t}\left[\boldsymbol{\varepsilon}_S\right] - {}^{t}\left[\boldsymbol{\varepsilon}_S\right] \\
\left[\Delta\boldsymbol{\varepsilon}_P\right] &= {}^{t+\Delta t}\left[\boldsymbol{\varepsilon}_P\right] - {}^{t}\left[{}^{m}\boldsymbol{\varepsilon}_P\right] \\
\left[{}^{m}\Delta\boldsymbol{\varepsilon}_S\right]^{0} &= \mathbf{A}:\left[{}^{f}\mathbf{C}^{T}_{SS}:\left[\Delta\boldsymbol{\varepsilon}_S\right] + {}^{f}k\left({}^{f}\mathbf{C}^{T}_{SP} - {}^{m}\mathbf{C}^{T}_{SP}\right) :\left[\Delta\boldsymbol{\varepsilon}_P\right]\right] \\
\text{where: } \mathbf{A} &= \left({}^{m}k\ {}^{f}\mathbf{C}^{T}_{SS} + {}^{f}k\ {}^{m}\mathbf{C}^{T}_{SS}\right)^{-1}
\end{aligned}
$$

- Finally, the initial value of the unknown $\left[{}^{m}\boldsymbol{\varepsilon}_S\right]^{k}$ is established.

$$
\left[{}^{m}\boldsymbol{\varepsilon}_S\right]^{k} = {}^{t}\left[{}^{m}\boldsymbol{\varepsilon}_S\right] + \left[{}^{m}\Delta\boldsymbol{\varepsilon}_S\right]^{0}
$$
$$
k = 0
$$

Step 2. Residue Evaluation.

The total strain tensors of the components $\left(\left[{}^{m}\boldsymbol{\varepsilon}\right]^{k}$ and $\left[{}^{f}\boldsymbol{\varepsilon}\right]^{k}\right)$ are determined as a function of the updated value of $\left[{}^{m}\boldsymbol{\varepsilon}_S\right]^{k}$.

$$
\left[{}^{m}\boldsymbol{\varepsilon}\right]^{k} = \left[{}^{m}\boldsymbol{\varepsilon}_P\right] + \left[{}^{m}\boldsymbol{\varepsilon}_S\right]^{k} \quad \text{where} \quad \left[{}^{m}\boldsymbol{\varepsilon}_P\right] = \left[{}^{f}\boldsymbol{\varepsilon}_P\right] = {}^{t+\Delta t}\left[\boldsymbol{\varepsilon}_P\right]
$$
$$
\left[{}^{f}\boldsymbol{\varepsilon}\right]^{k} = \left[{}^{f}\boldsymbol{\varepsilon}_P\right] + \left[{}^{f}\boldsymbol{\varepsilon}_S\right]^{k} \quad \text{where} \quad \left[{}^{f}\boldsymbol{\varepsilon}_S\right]^{k} = \tfrac{1}{{}^{f}k}\ {}^{t+\Delta t}\left[\boldsymbol{\varepsilon}_S\right] - \tfrac{{}^{m}k}{{}^{f}k}\left[{}^{m}\boldsymbol{\varepsilon}_S\right]^{k}
$$

The constitutive models of each material are checked to determine their updated internal variables and stress states.

$$
\underbrace{\left[{}^{m}\boldsymbol{\varepsilon}\right]^{k};\ {}^{t}\left[{}^{m}\alpha\right]}_{\Downarrow}
\qquad
\underbrace{\left[{}^{f}\boldsymbol{\varepsilon}\right]^{k};\ {}^{t}\left[{}^{f}\alpha\right]}_{\Downarrow}
$$
$$
\boxed{\begin{matrix}\text{Matrix}\\ \text{Model}\end{matrix}}
\qquad
\boxed{\begin{matrix}\text{Fibre}\\ \text{Model}\end{matrix}}
$$
$$
\Downarrow \qquad \Downarrow
$$
$$
\overbrace{\left[{}^{m}\boldsymbol{\sigma}\right]^{k};\ \left[{}^{m}\alpha\right]^{k}}
\qquad
\overbrace{\left[{}^{f}\boldsymbol{\sigma}\right]^{k};\ \left[{}^{f}\alpha\right]^{k}}
$$

Thereafter, the residue is evaluated to find out if the stress equilibrium (i.e., the convergence of the model) has been achieved.

$$\left[\Delta\boldsymbol{\sigma}_S\right]^k = \left[{}^m\boldsymbol{\sigma}_S\right]^k - \left[{}^f\boldsymbol{\sigma}_S\right]^k \quad \text{where:} \quad \left[{}^m\boldsymbol{\sigma}_S\right]^k = \mathbf{P}_S : \left[{}^m\boldsymbol{\sigma}\right]^k$$
$$\left[{}^f\boldsymbol{\sigma}_S\right]^k = \mathbf{P}_S : \left[{}^f\boldsymbol{\sigma}\right]^k$$

Step 3. Convergence Checking.

In order to choose the tolerance, the order of magnitude of the serial stresses must be considered as a reference. If the stresses of the previous step are different to zero, it is taken the minimum between them; on the contrary, the linearized stresses are taken as a reference.

$$ref1 = \min\left\{\left\| {}^t\left[{}^m\boldsymbol{\sigma}_S\right]\right\|, \left\| {}^t\left[{}^f\boldsymbol{\sigma}_S\right]\right\|\right\}$$
$$ref2 = \min\left\{\left\| {}^t\left[{}^m\mathbf{C}^T_{SS}\right] : \left[\boldsymbol{\varepsilon}_S\right] \right\|, \left\| {}^t\left[{}^f\mathbf{C}^T_{SS}\right] : \left[\boldsymbol{\varepsilon}_S\right] \right\|\right\}$$

$$\text{If} \quad ref1 > 0 \quad \text{then:} \quad refer = ref1$$
$$\text{else:} \quad refer = ref2$$

The tolerance is chosen based on the reference value:

$$toler = refer \cdot 10^{-4}$$

If the norm of the residue is greater than a tolerance, then to go to step 4 –correction of the unknown–, otherwise go to step 5 –update of variables–.

$$\text{If} \quad \left\|\left[\Delta\boldsymbol{\sigma}_S\right]^k\right\| > toler \quad \text{then:} \quad \text{goto Step 4.}$$
$$\text{else:} \quad \text{goto Step 5.}$$

Step 4. Correction of the Unknown.

Evaluation of tangent constitutive tensors of both materials.

The constitutive models of each material are evaluated to determine their tangent constitutive tensors.

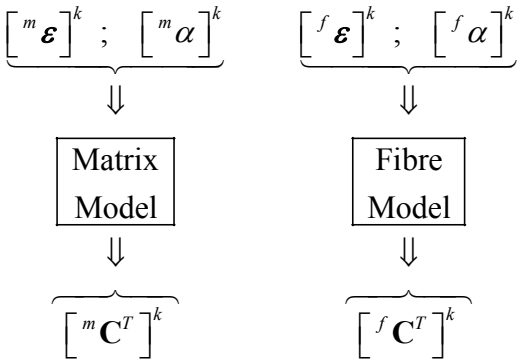

Calculation of the Jacobian.

$$\mathbf{J} = \left[{}^{m}\mathbf{C}^{T}_{SS} \right]^{k} + \frac{{}^{m}k}{{}^{f}k} \left[{}^{f}\mathbf{C}^{T}_{SS} \right]^{k} \quad \text{where:} \quad \left[{}^{m}\mathbf{C}^{T}_{SS} \right]^{k} = \mathbf{P}_{S} : \left[{}^{m}\mathbf{C}^{T} \right]^{k} : \mathbf{P}_{S}$$
$$\left[{}^{f}\mathbf{C}^{T}_{SS} \right]^{k} = \mathbf{P}_{S} : \left[{}^{f}\mathbf{C}^{T} \right]^{k} : \mathbf{P}_{S}$$

Update of the unknown.

$$\left[{}^{m}\boldsymbol{\varepsilon}_{S} \right]^{k} := \left[{}^{m}\boldsymbol{\varepsilon}_{S} \right]^{k} - \mathbf{J}^{-1} : \left[\Delta\boldsymbol{\sigma}_{S} \right]^{k}$$
$$k := k + 1$$

Go to step 2 –residue evaluation–.

Step 5. Update of Variables.

Once obtained the convergence of the constitutive model, all the variables of the model must be updated:

$$ {}^{t+\Delta t}\left[{}^{m}\boldsymbol{\varepsilon}_{S} \right] = \left[{}^{m}\boldsymbol{\varepsilon}_{S} \right]^{k} \quad ; \quad {}^{t+\Delta t}\left[{}^{m}\alpha \right] = \left[{}^{m}\alpha \right]^{k} \quad ; \quad {}^{t+\Delta t}\left[{}^{m}\boldsymbol{\sigma} \right] = \left[{}^{m}\boldsymbol{\sigma} \right]^{k}$$
$$ {}^{t+\Delta t}\left[{}^{f}\boldsymbol{\varepsilon}_{S} \right] = \left[{}^{f}\boldsymbol{\varepsilon}_{S} \right]^{k} \quad ; \quad {}^{t+\Delta t}\left[{}^{f}\alpha \right] = \left[{}^{f}\alpha \right]^{k} \quad ; \quad {}^{t+\Delta t}\left[{}^{f}\boldsymbol{\sigma} \right] = \left[{}^{f}\boldsymbol{\sigma} \right]^{k}$$

Step 6. Update of the Composite Stress State.

The stress tensor of the composite material is calculated taking into account equations (23), (24) and (17):

$$ {}^{t+\Delta t}\left[\boldsymbol{\sigma}\right] = {}^{m}k \; {}^{t+\Delta t}\left[{}^{m}\boldsymbol{\sigma}_{P} \right] + {}^{f}k \; {}^{t+\Delta t}\left[{}^{f}\boldsymbol{\sigma}_{P} \right] + {}^{t+\Delta t}\left[{}^{f}\boldsymbol{\sigma}_{S} \right]$$

The presented algorithm manages to compound of behaviours of materials fulfilling the hypotheses of the series-parallel problem. Note that the same algorithm may also deal with the extreme cases of pure serial or pure parallel behaviours.

3.6 Tangent Constitutive Tensor for the Composite

Once obtained the local convergence of the composite model (manager of constitutive models), it is necessary to find out the composite tangent constitutive tensor that will allow to achieve the convergence of the global problem.

In order to get this tangent tensor it is necessary to differentiate the composite stress tensor resulted form the solution of the linearized system of governing equations.

Note that in the linearization it is used the tangent constitutive tensors of the component phases ${}^{m}\mathbf{C}^{T}$ and ${}^{f}\mathbf{C}^{T}$ (provided by each simple model) which are based on the updated strain states and internal variables corresponding to each component.

$$ {}^{m}\mathbf{C}^{T} = {}^{m}g\left({}^{t+\Delta t}\left[{}^{m}\boldsymbol{\varepsilon} \right], \; {}^{t+\Delta t}\left[{}^{m}\alpha \right] \right) \tag{32}$$

$$ {}^{f}\mathbf{C}^{T} = {}^{f}g\left({}^{t+\Delta t}\left[{}^{f}\boldsymbol{\varepsilon} \right], \quad {}^{t+\Delta t}\left[{}^{f}\alpha \right] \right) \tag{33} $$

The expression of the algorithmic tangent tensor is obtained differentiating the composite stress tensor with respect to strain tensor in a way consistent with the integration algorithm:

$$ \mathbf{C}^{T} = \frac{\partial \boldsymbol{\sigma}}{\partial \boldsymbol{\varepsilon}} = \frac{\partial \Delta \boldsymbol{\sigma}}{\partial \Delta \boldsymbol{\varepsilon}} = \begin{bmatrix} \dfrac{\partial \Delta \boldsymbol{\sigma}_P}{\partial \Delta \boldsymbol{\varepsilon}_P} & \dfrac{\partial \Delta \boldsymbol{\sigma}_S}{\partial \Delta \boldsymbol{\varepsilon}_P} \\ \dfrac{\partial \Delta \boldsymbol{\sigma}_P}{\partial \Delta \boldsymbol{\varepsilon}_S} & \dfrac{\partial \Delta \boldsymbol{\sigma}_S}{\partial \Delta \boldsymbol{\varepsilon}_S} \end{bmatrix} = \begin{bmatrix} \mathbf{C}_{PP}^{T} & \mathbf{C}_{PS}^{T} \\ \mathbf{C}_{SP}^{T} & \mathbf{C}_{SS}^{T} \end{bmatrix} \tag{34} $$

where:

$$ \mathbf{C}_{PP}^{T} = \left({}^{m}k \; {}^{m}\mathbf{C}_{PP}^{T} + {}^{f}k \; {}^{f}\mathbf{C}_{PP}^{T} \right) \; + {}^{m}k \; {}^{f}k \left({}^{m}\mathbf{C}_{PS}^{T} - {}^{f}\mathbf{C}_{PS}^{T} \right) \; :\mathbf{C}: \left({}^{f}\mathbf{C}_{SP}^{T} - {}^{m}\mathbf{C}_{SP}^{T} \right) $$

$$ \mathbf{C}_{PS}^{T} = \left({}^{m}k \; {}^{m}\mathbf{C}_{PS}^{T} : \mathbf{A} : {}^{f}\mathbf{C}_{SS}^{T} + {}^{f}k \; {}^{f}\mathbf{C}_{PS}^{T} : \mathbf{A} : {}^{m}\mathbf{C}_{SS}^{T} \right) $$

$$ \mathbf{C}_{SP}^{T} = \left({}^{m}k \; {}^{f}\mathbf{C}_{SS}^{T} : \mathbf{A} : {}^{m}\mathbf{C}_{SP}^{T} + {}^{f}k \; {}^{m}\mathbf{C}_{SS}^{T} : \mathbf{A} : {}^{f}\mathbf{C}_{SP}^{T} \right) $$

$$ \mathbf{C}_{SS}^{T} = \tfrac{1}{2} \left({}^{m}\mathbf{C}_{SS}^{T} : \mathbf{A} : {}^{f}\mathbf{C}_{SS}^{T} + {}^{f}\mathbf{C}_{SS}^{T} : \mathbf{A} : {}^{m}\mathbf{C}_{SS}^{T} \right) $$

$$ \text{with: } \mathbf{A} = \left({}^{m}k \; {}^{f}\mathbf{C}_{SS}^{T} + {}^{f}k \; {}^{m}\mathbf{C}_{SS}^{T} \right)^{-1} $$

It can be clearly observed that the expression of the composite tangent tensor $\mathbf{C}^{T}$ maintains its symmetry when the tangent tensors of components (${}^{m}\mathbf{C}^{T}$ and ${}^{f}\mathbf{C}^{T}$) are also symmetrical.

3.7 Enrichment of the Transversal Behaviour

The assumption of equal stress in orthogonal directions to the fibre (pure serial behaviour in transverse directions), constitute a lower bound for the transverse stiffness of the composite. Experimental results confirm this fact (see next figure). For this reason, an enrichment in the proposed numerical model is required to be able to predict the transversal behaviour more accurately. That is, the Basic SP model is upgraded into the Enriched Serial-Parallel model (ESP model).

In order not to resort to a more complex model, an improvement is performed that maintains the structure of the previously developed algorithm: the behaviour of the most deformable material (matrix) is stiffened by means of a gamma parameter. The structure of the new algorithm is similar to the previous one, being its only difference the use of $\left({}^{m}\boldsymbol{\varepsilon} \right)^{*}$, $\left({}^{m}\boldsymbol{\sigma} \right)^{*}$, $\left({}^{m}\mathbf{C}^{T} \right)^{*}$ instead of ${}^{m}\boldsymbol{\varepsilon}$, ${}^{m}\boldsymbol{\sigma}$, ${}^{m}\mathbf{C}^{T}$, whose expressions are:

$$ \left({}^{m}\boldsymbol{\varepsilon} \right)^{*} = \left[{}^{m}\mathbf{K} \right]^{-1} : {}^{m}\boldsymbol{\varepsilon} \tag{35} $$

$$ \left({}^{m}\boldsymbol{\sigma} \right)^{*} = {}^{m}\mathbf{K} : {}^{m}\boldsymbol{\sigma} \tag{36} $$

$$ \left({}^{m}\mathbf{C}^{T} \right)^{*} = {}^{m}\mathbf{K} : {}^{m}\mathbf{C}^{T} : {}^{m}\mathbf{K} \tag{37} $$

$$\text{where:} \quad {}^{m}\mathbf{K} = \mathbf{P}_P : \mathbf{I} : \mathbf{P}_P + {}^{m}\gamma \ \mathbf{P}_S : \mathbf{I} : \mathbf{P}_S$$

By means of micro-mechanical considerations it is possible to take values of the gamma parameter as a function of the fibre volumetric fraction $\left({}^{f}k\right)$ and the ratio between fibre and matrix Young modules $\left(R = {}^{f}E / {}^{m}E\right)$ (see Figure 3). For example: ${}^{m}\gamma = 1.31$ for $R = 20$ and ${}^{f}k = 0.6$.

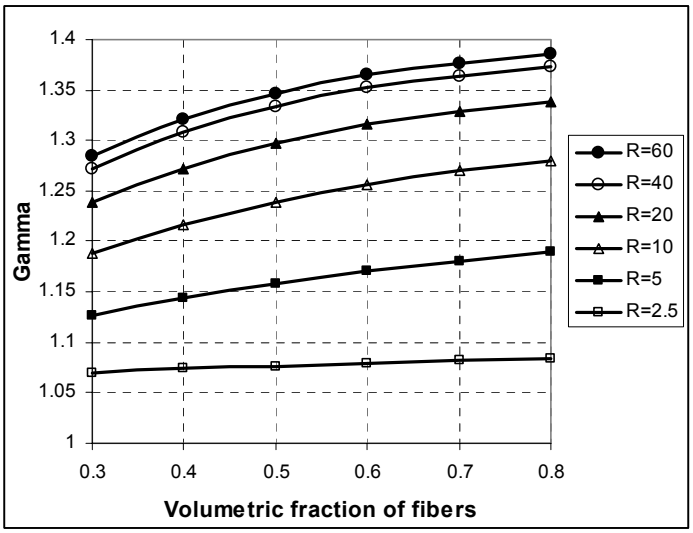

Figure 3: Estimative values of gamma as a function of the fibre volumetric fraction for different stiffness ratios.

In the following, the predictive capacity of pure Serial-Parallel (SP) model and enriched SP model for the transversal stiffness of a glass-epoxy lamina with E_F/E_M=21.19, ν_F=0.22, ν_M=0.38 (stiffness ratio and Poisson ratios) is compared against experimental data and against the estimation given by broadly used semi-empirical formulas. An hexahedral composite element is subjected to pure transversal load, at different fibre volume fractions. In Figure 4, the adimensional curves E_2/E_m vs. ${}^{f}k$ resulting from numerical simulations are given together with experimental values taken from Barbero [10] (pag. 72). The curves resulting from perfect inverse R.O.M. and from Halpin-Tsai equation are also given in the same figure.

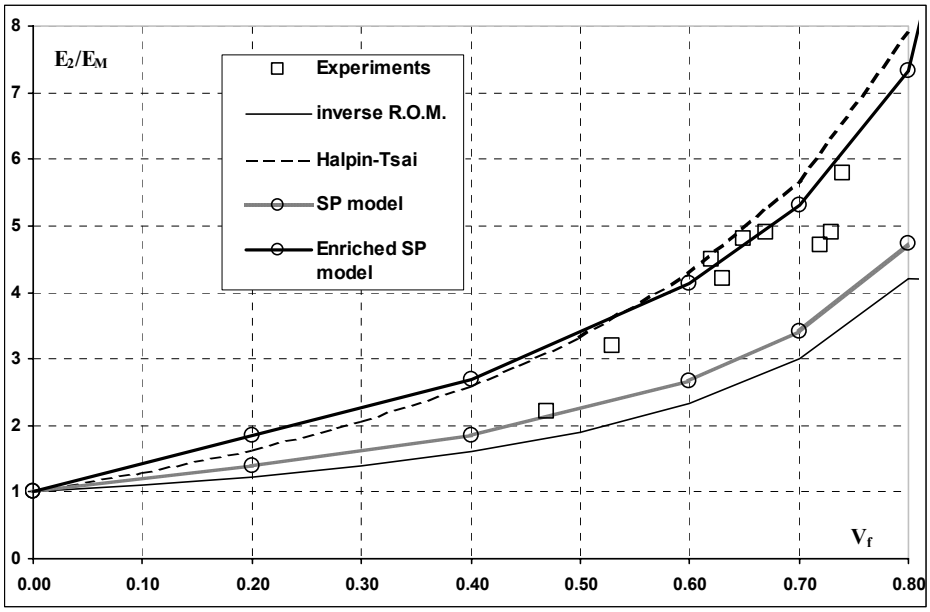

Figure 4: Relative transversal stiffness of a glass-epoxy lamina as a function of fibre volume fraction. Numerical results compared against experimental data and against estimations given by broadly used semi-empirical formulas.

The transversal stiffness obtained by pure SP model results to be slightly greater than the one given by inverse ROM, due to Poisson effects. Of course, when Poisson ratios are set equal to zero a perfect inverse ROM curve is recovered.

The graph shows that simple SP model, as well as inverse ROM, underestimates the experimental values. On the other side enriched SP model, with an appropriate gamma, obtains an approximation to experimental data as good as the one given by Halpin-Tsai equation.

4.0 CALIBRATION AND VALIDATION OF THE MODEL

The numerical model proposed to simulate the behaviour of composite materials is based on the appropriate management of the constitutive models of the different component materials considering the morphology and distribution of fibres within the matrix [2].

Some mechanical parameters, such as the transverse Young's modulus for anisotropic fibres (e.g.: carbon fibres), are impossible to obtain by means of direct measurements. Therefore, it must be deduced indirectly by means of calibration of this parameter to fit the stiffness of the lamina, or by means of a formula that considers the transverse Young modulus of the composite, the Young modulus of the matrix and the volumetric participation of the fibre [10]. Once these parameters are determined they remain linked to that component material since they are its attribute; they are independent of fibres direction, their volumetric participation, the loads or the kind of problem.

In order to study the fatigue phenomenon in composed materials, it is necessary to calibrate the parameters that determine the life curves S-N of the matrix and of the fibre, with the tests done on laminas of composite. Then, the tests on laminates and structures will allow verifying if the calibration has been made successfully.

As calibration methodology for the fatigue phenomenon, the following tips set out:

- calibrate the life curve S-N of the matrix with fatigue tests done on laminas with fibres at 90 degrees;
- calibrate the life curve S-N of the fibre with fatigue tests done on laminas with fibres at 0 degrees;
- verify that the calibrations respond to the behaviour of laminas at 90 degrees; failing that, return to the first step;
- verify with the response of the fatigue tests done on [+45/-45]sym laminates; failing that, it will be necessary to include an interphase "material" and to calibrate it (currently the model does not include the interface since perfect adhesion between fibre and matrix is assumed, but this one could be taken into account by means of slight changes in the strain compatibility equations);
- verify the values with other laminates and/or structures.

The model is validated with experimental testing done at 'Institute for Static and Dynamics' (ISD) of University of Stuttgart on CFRR material samples. Carbon fibre here is Tenax HTA 5241 and the resin used is Ruetapox VE4434. Values for mechanic properties of components have been given by manufacturers and they are listed in Table 1.

Table 1: Materials mechanical properties given by manufacturers

Components Properties	Unit	Fibres values	Resin values
Density (m_c)	kg/m3	1770	1092
Tensile strength	MPa	3950	
Tensile strain	%	1.5	
Young's modulus parallel	GPa	238	4
Young's modulus perpendicular	GPa	28	4
Shear modulus	GPa	50	1.5
Poisson's ratio (ν_{xy})	-	0.23	0.35
Mass (M_c)	g	3.771	2.381
Volumetric content ratio (k_c)	-	0.4942	0.5058

The lay-up has been chosen to get a symmetric laminate configuration.

- 3-layer specimen [0 90 0] [90 0 90] [0 90 0]
- 4-layer specimen [90 0 90] [45 -45 45] [45 -45 45] [90 0 90]
- 5-layer specimen [90 0 90] [45 -45 45] [90 0 90] [45 -45 45] [90 0 90]

The thickness of the laminas is chosen in such a way that the numbers of fibres are the same in both directions, inner layers twice thick as the outer ones.

Static testing: For each type of specimen (3, 4, 5-layers) five force controlled tensile test (European Standard EN 2561) have been carried out to find out the Young's modulus, the Poisson's ratio and the ultimate strength (stress at load to fracture).

Figures 5 and 6 show the comparison between experimental results and numerical simulations for the 3-layer specimens at 0º and 45º loading directions. Looking at the break pattern of the specimens it can be seen that

failure is caused by fracture of fibres in the 0º loading direction (quasi-linear stress-strain curve) and due to shear failure of the matrix in the 45° case (strong non-linear stress-strain curve). Both situations are accurately reproduced by the numerical simulations.

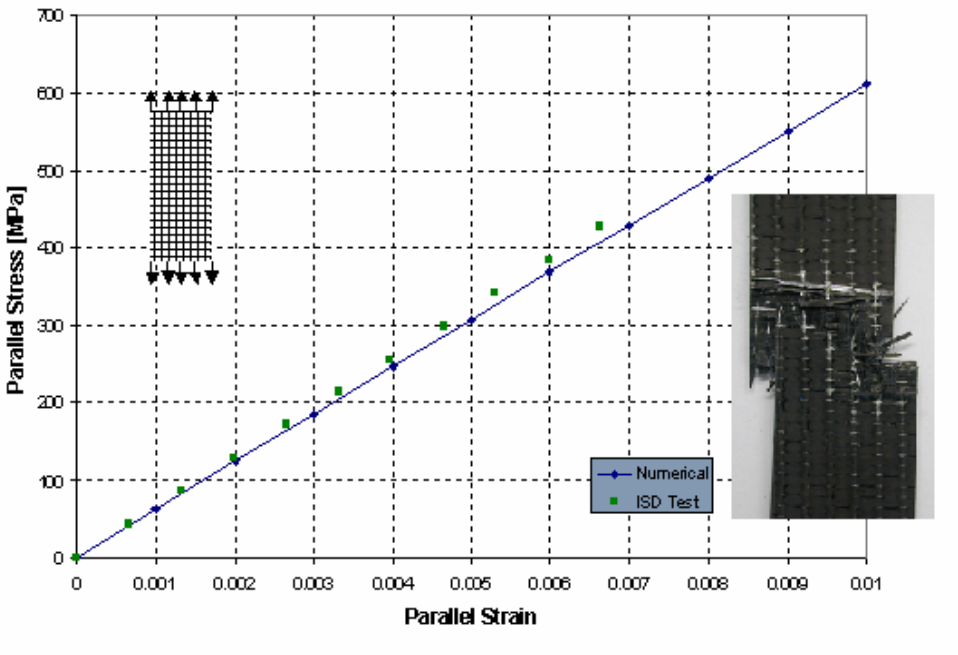

Figure 5: Tensile Strength Test - 3-layer specimen [0 90 0] [90 0 90] [0 90 0].

Dynamic testing: Tension cyclic loading with a ratio S_{min}/S_{max} = 0.1 and maximum stress depending on the thickness of the samples have been used for durability tests. For 3-layered specimens, load levels of 440, 480 and 500 MPa are applied up to failure. The damage progress within the inspected specimens are observed in different ways: Stiffness monitoring (stiffness decrease is a concomitant of damage progress), hysteresis measurement (dissipated energy equivalent to area of hysteresis loop and damage progress) and heat radiation. In Figure 7 (left side) resulting stiffness plots over the number of load-cycles for different load-levels are summarized. On the right side of Fig. 7 the corresponding results of numerical simulations are presented. Good agreement is found for the 440 MPa load case, acceptable for the 480 MPa case and it is difficult to assert about the 500 MPa loading case. Looking at the experimental results for the three different load-levels a significantly increasing variation of the number of load-cycles to failure can be observed.

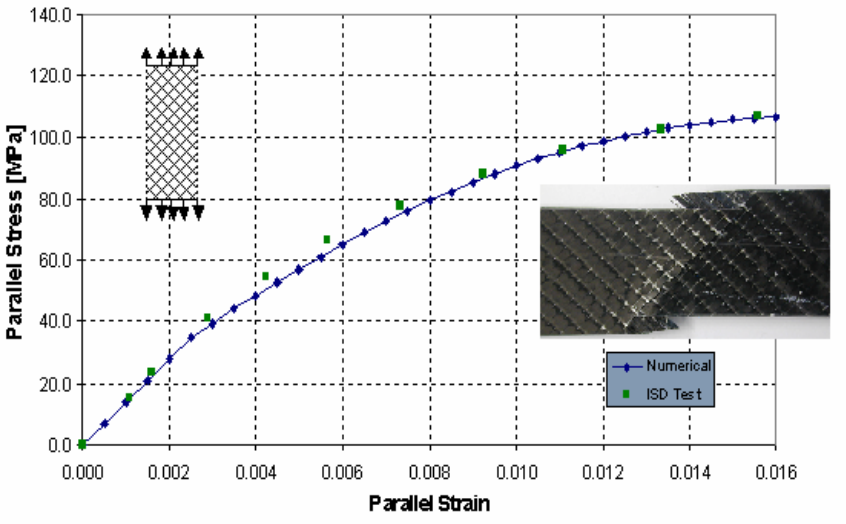

Figure 6: Tensile Strength Test - 3-layer specimen [45 -45 45] [-45 45 -45] [45 -45 45].

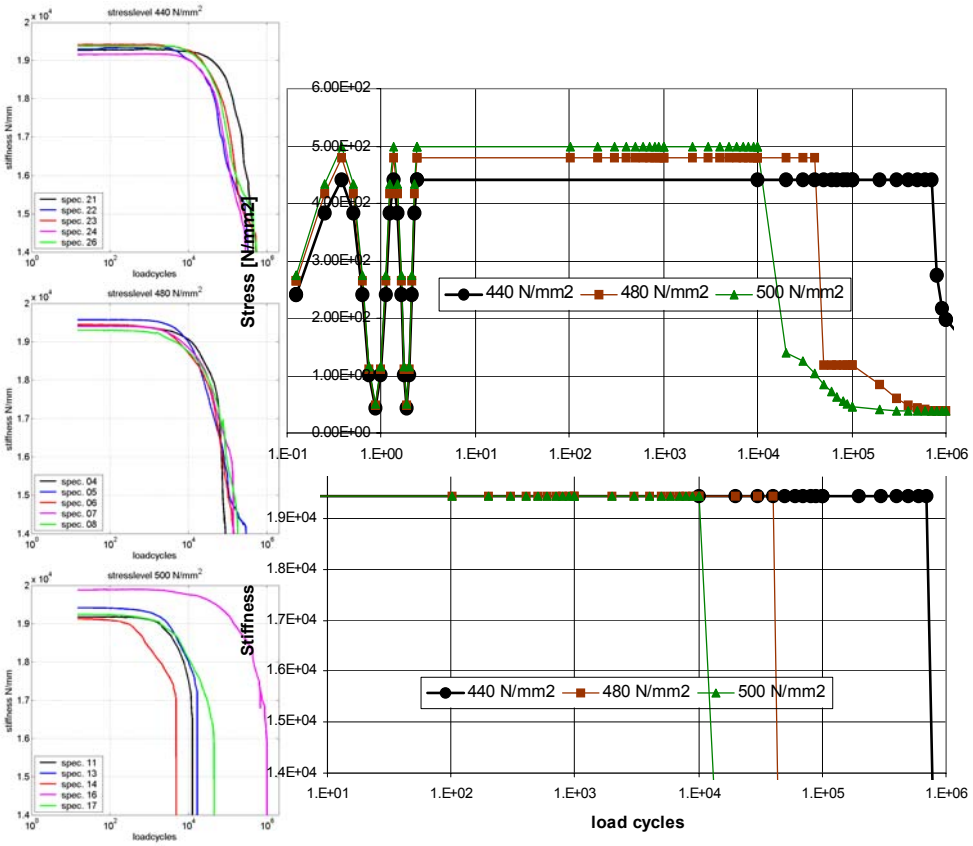

Figure 7: Fatigue behaviour of 3-layer specimens. Experimental results on the left, numerical simulations on the right.

5.0 CONCLUSIONS

The Serial-Parallel (SP) model is combined with classical lamination theory to describe laminates consisting of unidirectional continuously reinforced layers. Its relative simplicity and the resulting numerical efficiency make the SP approach well suited for implementation as a material model in Finite Element programs for studying the elastoplastic response of structures or components made of continuously reinforced or laminated composites. In addition, it requires relatively small computational resources when implemented into a structural FE code. Its initial drawback of underestimation of the transverse and shear stiffness, is then improved upon with the Enriched SP model.

A fatigue model based on continuum mechanics accounting for elasto-plastic-damage constitutive equations, previously developed by the authors, has been applied to the components of CFRR material in order to obtain the durability of the whole composite laminate. Comparison between experimental and numerical testing carried out on material samples allow saying the methodology presented here is very promising for durability analysis of composite materials and structures.

ACKNOWLEDGMENTS

This work has been partially funded by European Commission under the GROWTH Project GRD2-2000-30091, COMPASS, Contract G5RD-CT-2001-00575 and by the Spanish government through FPU grant for F. Rastellini. This support as well as the experimental results obtained by Dr. C. Hofmann at Institute for Static and Dynamics (ISD), University of Stuttgart is gratefully acknowledged. We are indebted to R. Serpieri for his help on the numerical model validations.

REFERENCES

[1] Oller, S; Salomon, O.; Oñate, E. (2005). A continuum mechanics model for mechanical fatigue analysis. Computational Materials Science 32, 175–195

[2] Rastellini, F.; Oller, S. (2004). Modelado numérico de no linealidad constitutiva en laminados compuestos - Teoría de mezclas. Métodos Computacionais em Engenharia. Lisboa (Portugal): APMTAC.

[3] Rastellini, F.; Oller, S.; Salomon, O.; Oñate, E. (2003). “Teoría de Mezclas Serie-Paralelo Avanzada para el Análisis de Materiales Compuestos” V Congreso de la Asociacion Española de Materiales Compuestos, © AEMAC, 2003, pág. 729-741. ISBN 84-9213-49-8-4 A. Mirevete & J. Cuartero (Eds)

[4] Rastellini, F.; Oller, S.; Salomon, O.; Oñate, E. (2003). “Advanced serial-parallel mixing theory for composite materials analysis. Continuum basis and finite element applications”, COMPLAS 2003, Proceeding (CD) of the VII International Conference on Computational Plasticity ISBN: 84-95999-22-6 CIMNE, Barcelona.

[5] Salomon, O.; Oller, S.; Oñate, E. (2002) “Industrial Application of Fatigue Damage Analysis and FEM”, NAFEMS-FENET Technology Workshops. Durability and Life Extension. Zurich(Geroldswill), Switzerland.

[6] Salomon, O.; Oller, S.; Oñate, E. (2002) “Fatigue Damage Modelling and Finite Elements Analysis Methodology: Continuum Basis and Applications”, FATIGUE 2002, Proceeding of the Eighth International Fatigue Congress, Ed. A.F.Blom, Stockholm, Sweden, pag. 2689-2696, Vol.4/5

[7] Salomon, O.; Oller, S.; Oñate, E. (2002) "Fatigue Analysis of Materials and Structures using a Continuum Damage Model", International Journal of Forming Processes, Vol. 5, Nº 2-3-4, Pgs.493-503, 2002. Ed. HERMES Science Publications, France

[8] Y.A. Bahei-el-Din. Plastic Analysis of Metal Matrix Composite Laminates, Doctoral Thesis, Duke University, Durham, NC, 1979.

[9] G.J. Dvorak, Y.A. Bahei-el-Din. Plasticity analysis of fibrous composites, J. Appl. Mech. 49, 327-335, 1982.

[10] Barbero, E. J. (1998). Introduction to composite materials design. London: Taylor & Francis.

SYMPOSIA DISCUSSION – PAPER NO: 31

Author's name: O. Salomon

Discussor's name: J. Calcaterra

Question: In the continuum fatigue formulation, you assumed a fatigue endurance limit stress- Are there data to validate this assumption for your material?

Answer: For composite materials experimental data corresponding to components must be obtained from tests on the final material (composite) using special configurations and 'known' data for one of the composites. This is not an easy task but can be done. Anyway, a 'fixed' stress endurance limit is not a requirement for the model. If stress continues decreasing as a function of number of cycles, this information is the important. There is no need for a constant endurance limit.